Journal of CO2 Utilization 78 (2023) 102634

Contents lists available at ScienceDirect

Journal of CO2 Utilization

journal homepage: www.elsevier.com/locate/jcou

# Power to gas and top gas recycling integration in an oxygen blast furnace steelmaking industry

Jorge Perpiñán [a,*], Manuel Bailera [a], Begoña Peña [a], Pravin Kannan [b], Valerie Eveloy [b], Luis M. Romeo [a]

[a] Escuela de Ingeniería y Arquitectura, Universidad de Zaragoza, María de Luna 3, 50018 Zaragoza, Spain
[b] Khalifa University, Department of Mechanical Engineering, United Arab Emirates

ARTICLE INFO

*Keywords:*
Low-carbon steel
Power-to-Gas
Methanation
Amine scrubbing
Decarbonization

ABSTRACT

A new process concept integrating power to methane with top gas recycling in an oxygen blast furnace (BF) is investigated to reduce the emission intensity of steelmaking. Power to gas produces synthetic methane using hydrogen ($H_2$) generated by an electrolyser operated with renewable electricity, and $CO_2$ captured from the BF gas by amine scrubbing supplied with heat from the methanation process. The clean gas from the amine scrubbing is recycled and injected in the BF (via top gas recycling), together with synthetic methane. A parametric analysis is performed to vary the amount of top gas recycled (from 0 kg/tHM to 270 kg/tHM). Based on the results, $CO_2$ equivalent emissions can decrease by 34% using power to gas technology, and by 30% with power to gas and top gas recycling (compared to conventional BFs). Nevertheless, if both integrations are present, additional benefits on the specific energy consumption (12.0 MJ/$t_{HM}$), and specific cost (130 €/$t_{HM}$) are achieved, compared to only applying power to gas (17.5 MJ/$t_{HM}$ and 233 €/$t_{HM}$). In all cases, the downstream thermal energy needs of the steel plant are fulfilled, contrarily to conventional top gas recycling concepts. The main conclusion is that top gas recycling should be considered together with PtG technology, and vice versa, when integrated in blast furnace ironmaking, in order to both abate emissions while supplying downstream energy needs.

## Nomenclature

| | |
|---|---|
| AFT | Adiabatic Flame Temperature |
| ASU | Air Separation Unit |
| AHF | Air Heating Furnace |
| BF-BOF | Blast Furnace-Basic Oxygen Furnace |
| BFG | Blast Furnace Gas. |
| BOFG | Basic Oxygen Furnace Gas |
| CC | Carbon Capture |
| CCS | Carbon Capture Storage |
| COG | Coke Oven Gas |
| DRI | Direct Reduced Iron |
| EAF | Electric Arc Furnace |
| GHG | Green House Gas |
| HM | Hot Metal |
| I&S | Iron and Steel |
| IEA | International Energy Agency |
| LHV | Lower Heating Value |
| MDEA | Methyldiethanolamine |
| PEM | Proton Exchange Membrane |
| PtG | Power to Gas |
| PCI | Pulverised Coal Injection |
| PFD | Process Flow Diagram |
| SNG | Synthetic Natural Gas |
| tHM | Ton of Hot Metal |
| tCS | Ton of Crude Steel |
| TGR | Top Gas Recycling |
| α,β,γ | Parameters for Economic Analysis |

## 1. Introduction

Annual $CO_2$ emissions from the iron and steel (I&S) industry have increased over the past decade by ~31% [1], primarily due to increased demand for steel production, and currently represent almost 25% of all

* Corresponding author.
*E-mail address:* jorge.perpinan@unizar.es (J. Perpiñán).

https://doi.org/10.1016/j.jcou.2023.102634
Received 5 May 2023; Received in revised form 25 October 2023; Accepted 23 November 2023
Available online 28 November 2023

industrial emissions (~2.6 Gt of $CO_2$) [2]. In order to limit global warming to below 1.5 °C, the I&S industry will require a portfolio of low-carbon technologies, including renewable electricity, hydrogen ($H_2$), and carbon capture (CC), especially in the medium term, when direct abatement technologies not yet deployed at sufficient scales [2].

The blast furnace-basic oxygen furnace (BF-BOF) is the dominant primary steel production route [3] and the most energy-intensive, utilizing 20–30 GJ/$t_{LS}$ [1]. Conventional coal/coke-based BF-BOF processes utilize ~800 kg of coal and emit ~1.8–2.2 $t_{CO2}/t_{LS}$ [2], with two thirds of these emissions incurred in the BF [4]. Molten metal is formed in the BF through reduction of iron and accompanying elements from their oxides, and refined in the BOF to produce crude liquid steel [5]. Typical reducing agents include coke formed after carbonization of coal in coke oven, pulverized coal (PC), and natural gas (NG). Complete reduction of iron ore (mainly hematite $Fe_2O_3$ and magnetite $Fe_3O_4$) is accomplished by a combination of indirect reduction with CO and $H_2$ and direct reduction with carbon [6,7] (Table 1).

The evolution of the BF process, illustrated in Fig. 1, is characterized initially by a decrease in coke rate utilization, followed by several technology improvements, especially on the composition of the blast, to reduce carbon consumption [8], [9]. In the early years (1960's), the traditional blast furnace (BF) employed a combined blast of hot air and oil to supply energy for iron ore reduction reactions. Following the subsequent oil crisis, the blast oil was substituted with PC and enriched $O_2$ towards coke-only operation. During the transition period, approaches to reduce coke consumption using reducing gas produced by reforming either oil or NG, or using coke oven gas were explored. Although these process modifications did not lead to commercialization, they enabled the development of various oxygen blast furnace (OBF) variants during the 1980's that sought to significantly reduce carbon consumption. These variants employed a combination of pre-heat gas and blast furnace gas (BFG) exhaust injection back into the BF after $CO_2$ capture, using various process configurations. Subsequently, an advanced OBF process utilizing intensified NG injection in a downsized BF, was proposed to reduce carbon input and energy penalty. Among notable OBF variants, the oxygen BF with top gas recycling (OBF-TGR) using carbon capture and storage (CCS), and the advanced OBF, have enabled a coke rate reduction to 200–300 kg/$t_{HM}$, from 330 to 400 kg/$t_{HM}$ in the traditional BF process, and thus have been considered a significant technological improvement for energy savings and emission reductions [10], [11]. Key research efforts that have addressed OBF development, OBF integration with TGR, OBF integration with CCS, and OBF integration with Power to Gas (PtG) are reviewed as follows.

The OBF involves injection of either medium $O_2$-enriched (30–60% $O_2$) or full-oxygen (>90% $O_2$) blast furnace, instead of slightly-rich $O_2$ blast in the traditional BF (<30%). The $O_2$-enriched air enhances partial combustion of coke and auxiliary fuels, thereby generating a $N_2$-deficit top gas, comprising mainly of CO, $CO_2$, $H_2$ and $H_2O$ [12]. A higher $O_2$ content in the blast enables injection of large amounts of PC [9], and thus increases productivity. On the other hand, gas injection as a supplementary reducing agent lowers the direct reduction ratio, and promotes low carbon consumption. Among the different gaseous injectants tested, NG has been found to be the most effective in significantly curtailing coke rate for a specified injection volume [9]. Zhang et al. [11]

**Table 1**
Typical reduction reactions of iron ore in a blast furnace [6,7].

| Reaction | Equation | No. |
|---|---|---|
| Indirect reduction by CO | $3Fe_2O_3(s) + CO(g) \rightarrow 2Fe_3O_4(s) + CO_2(g)$ | (1) |
| | $Fe_3O_4(s) + CO(g) \rightarrow 3FeO(s) + CO_2(g)$ | (2) |
| | $Fe_3O_4(s) + 4CO(g) \rightarrow 3Fe(s) + 4CO_2(g)$ | (3) |
| | $FeO(s) + CO(g) \rightarrow Fe(s) + CO_2(g)$ | (4) |
| Indirect reduction by $H_2$ | $3Fe_2O_3(s) + H_2(g) \rightarrow 2Fe_3O_4(s) + H_2O(g)$ | (5) |
| | $Fe_3O_4(s) + H_2(g) \rightarrow 3FeO(s) + H_2O(g)$ | (6) |
| | $FeO(s) + H_2(g) \rightarrow Fe(s) + H_2O(g)$ | (7) |
| Direct reduction of liquid FeO | $FeO(l) + C(s) \rightarrow Fe(l) + CO(g)$ | (8) |

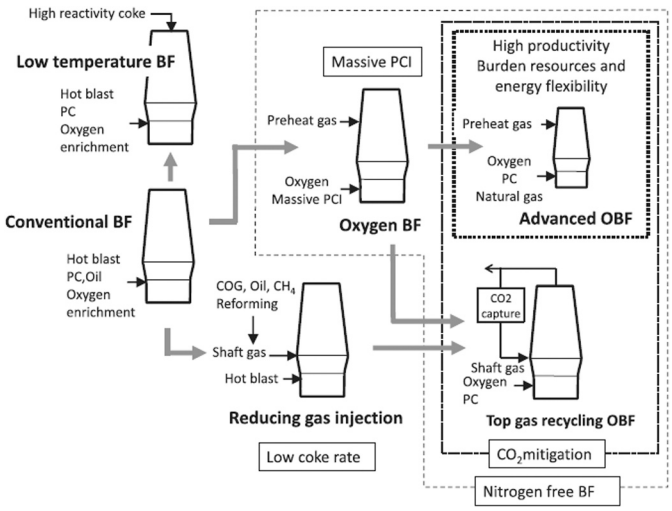


**Fig. 1.** Evolution of BF technology for diminishing coke rate and $CO_2$ emissions. PC – Pulverized coal.
Adapted from [8].

reviewed the evolution of OBF with particular focus on gas injection point and process characteristics. OBF development has particularly focused on minimizing spatial temperature gradients between the upper and lower regions of the OBF.

The concept of integrating the OBF with TGR has been studied comprehensively in recent years [8,9,11,13–19]. The primary goal of TGR is to decrease the carbon input by partially substituting PC with unused CO and/or $H_2$ in the top gas after $CO_2$ capture. In this context, different OBF-TGR process designs have been proposed depending on the point where recycled gas is introduced into the BF, or whether $CO_2$ is captured from the exhaust before recycling the top gas [8,9,11,15,16,19]. The recycled gas could be introduced back into the BF either through the hearth tuyeres, mid shaft, upper tuyeres, or a combination of these [20]. The first industrial trial of the OBF process (NKK-OBF) employed TGR without $CO_2$ sequestration [11]. In this process, a part of the recycle stream was split between hearth tuyeres and mid-shaft, and the remaining exported for utilization. The results demonstrated a significant decrease in coke rate (and thus total fuel rate) due to the increase in the amount of PC injected [11]. Another industrial Tula-OBF process employed $CO_2$ capture before a part of treated blast furnace gas (BFG) was preheated and introduced into the hearth tuyeres along with full $O_2$ blast [11]. Although successful in reducing the coke injection rate, technical difficulties were encountered in the process due to prolonged operation of the OBF with low coke flowrate and low $O_2$ blast velocity. In a more recently developed TGR-OBF process within ULCOS project, recycling of $CO_2$-deprived top gas at both hearth and shaft sections of the BF was considered, after preheating the recycled gas to different temperatures using a blast mixture of cold $O_2$ and PC [11], [18]. The results showed that combined injection of recycle gas into hearth led to lower coal and coke consumption compared to injection at hearth alone. Also, 76% reduction in $CO_2$ emissions (24% mitigation by gas recycling, and 52% by $CO_2$ extraction) was found to be potentially achievable using the proposed configuration [21]. Other studies that have investigated similar process designs have proposed combusting a part (~10%) of raw BFG to supply heat for pre-heating the recycled shaft or tuyere gas stream [19], [22], [23]. Some alternative OBF design features include a pre-heated injection stream, wherein a fraction of raw BFG is pre-heated to ~1000 °C and introduced into the upper shaft of the BF [24]. The results showed that the auxiliary stream assisted in improving the heat distribution throughout the upper shaft, and the pre-heating gas composition and flow had minimal impact on the reduction reactions in the lower shaft [24].

Integration of the OBF and TGR can synergetic act towards carbon

mitigation. For instance, an integrated steel mill operated with the OBF-TGR process was found to significantly curtail $CO_2$ emissions (ca. 43%) relative to a traditional BF steel mill [22], [23]. Other benefits over the OBF-TGR include: high productivity, reduced fuel rate (due to increase in indirect reduction degree), improved top gas calorific value (and thus reduced energy demand), improved bed fluidization (and thus productivity), reduced environmental impact, and improved PC injection rate (and thus reduced dependence on metallurgical coke) [11], [21], [24], [25]. Although $O_2$ consumption in the OBF is significantly higher than in the traditional BF process (220 $Nm^3/t_{HM}$ vs. 70 $Nm^3/t_{HM}$ [22]), the additional $O_2$ supply could be sourced from the existing air separation unit in traditional BF. One of the main challenges in deploying TGR in OBF is unavailability of sufficient energy for downstream processes due to top gas recycling and subsequent reduced carbon input [9], [14]. Depending on the recirculating ratio of the top gas, which typically ranges between 30% and 100% [20], the process would incur a thermal energy penalization of 1.5–4 $GJ/t_{HM}$ [9]. Integrating the TGR process with a low-carbon source such as NG instead of PC has been found to increase the calorific value of the BFG by ~2 times relative to traditional BF [8], and thus has been recommended as a potential solution [9].

It should be noted that recycling part of the BFG exhaust with high $CO_2$ and $H_2O$ content into the tuyeres would not be desirable, as this tends to increase coke consumption and impedes reduction reactions of iron oxides [20]. Thus, the TGR process is usually accompanied by CC and steam condensation prior to recycling the gases into the furnace. The benefits of integrating CCS with an OBF-TGR steel mill has been realized in industrial trials [19], [22], [23]. In comparison to the traditional BF, the overall $CO_2$ emissions reduction was estimated to reach ~88%, and thus the integration has been envisaged as the only technological pathway for reducing on-site emissions from integrated steel mills [22]. Quader et al. [13] evaluated different criteria for CCS technology selection for a specific iron and steel process, and identified energy for capture and storage, and $CO_2$ removal efficiency as the two key factors. Vacuum pressure swing adsorption (VPSA) and amine scrubbing are the most common $CO_2$ capture techniques employed in BF-BOF processes based on previous works by [26–34]. The primary drawbacks of amine scrubbing are degradation of the solvent (which thus requires replacement), and the need for a significant amount of steam for solvent regeneration, ~2–4 $GJ/t_{CO2}$ of thermal energy (equivalent electricity penalty of ~0.7–1.4 $GJ/t_{CO2}$) [9], [35]. However, as the BFG contains minimal amounts of $O_2$, the amines would be less susceptible to degradation, making amine absorption technique suitable for $CO_2$ capture from the BF top gas. Among the solvents tested for $CO_2$ absorption performance, monoethanolamine (MEA) has been found to be the ideal candidate, despite the high regeneration energy [26,28]. This is due to the ability of MEA to regenerate at a lower temperature using low exergy heat that is widely available in steel site. Moreover, the differences in $CO_2$ recovery ratio between MEA and advanced solvents were not found to be significant. Although some solvent blends have been found to exhibit improved performance [32], the results have been limited to simulation studies.

Combining OBF and PtG has been recently proposed to promote carbon recycling within steel production facilities [36]. Rosenfeld et al. [37] and Medved [38] analysed different configurations of PtG with biomass methanation, and Hisashige et al. [39] studied a combination of TGR with a SOEC electrolyser. Other authors injected pure $H_2$ in the furnace, either from a low temperature electrolyser (PEM or Alkaline) [40] or from a high temperature electrolyser (SOEC) [41]. Utilizing renewable energy for water electrolysis, PtG technology generates $H_2$ that is combined with either carbon-rich exhaust gases [42], [43] or treated BFG [17], [20], [44] from the ironmaking process to generate synthetic methane or SNG and effectively replace NG. Following a comprehensive analysis of various PtG options, it has been concluded that PtG using treated BFG offers the highest $CO_2$ reduction potential [42]. The amount of $CO_2$ emissions that can be avoided by PtG integration is limited by the maximum volume of SNG that can be injected in the BF, which depends on the flame temperature. Approximately, up to 200–500 $kg/t_{HM}$ of $CO_2$ (equivalent to 15–40% of the emissions of a traditional BF) could be retained in closed loop recycling and avoided from being permanently stored [42], [45]. However, this approach implies an additional electricity penalization of ~1.3–2.1 $GJ/t_{HM}$ for the production of renewable $H_2$ [36].

In previous work, we developed and validated a reference model for the conventional iron and steel plant [43]. Building on this foundation, in this paper, we present a novel integration model that combines Power to Gas technology in the iron and steel industry. Specifically, while our previous work focused on Power to Gas in an air-blown blast furnace (9.4% of carbon avoidance and 283 €/$t_{CO2}$ of carbon avoidance cost) [43], and on the influence of the oxygen enrichment and its temperature in the hot blast (34% of carbon avoidance and 352 €/$t_{CO2}$ of carbon avoidance cost) [45], the new integration model operates with Top Gas Recycling in an oxygen blast furnace, to achieve lower energy consumption and costs while maintaining a high carbon avoidance rate.

Therefore, the present work seeks to assess the performance and cost of a power to gas installation in an oxygen blast furnace ironmaking plant and its coupling with top gas recycling technology. The novelty of the study relies on the synergetic injection of $CO_2$-free top gas (clean-BFG or TGR gas) and intensified SNG in an advanced OBF process, which has not been explored earlier. Moreover, the effects of complete substitution of the PC with SNG on the techno-economic performance of an OBF, for which understanding is at present limited, are investigated. Accordingly, through the present investigation, we intend to develop an improved "closed-loop" strategy for carbon recycling within BF operation based on an integrated PtG and OBF-TGR process model. The outcome of this study will detail the significance of integration and assess the influence of the top gas recycling ratio, and recycling gas composition on the specific energy consumption and cost of steel production.

## 2. Process configurations

In this study, a new process configuration that integrates Power to Gas technology with the steelmaking process is investigated having the potential to lead to significant reductions in energy consumption and costs, without compromising the high carbon avoidance rate. This configuration is compared with a reference case that serves as a baseline for comparison, and has been previously detailed, modelled and validated [43].

The proposed PtG-steelmaking integration with top gas recycling (TGR) and oxy-BF is presented in Fig. 2, where the dashed lines represent the additional streams and blocks needed to carry out the PtG integration. This case includes several blocks, such as the PEM electrolyser for $H_2$ production, amine scrubbing for $CO_2$ capture, and methanation plant for synthetic natural gas (SNG) production. Moreover, it modified the BF to an oxy-BF (i.e., pure oxygen is supplied instead of air). The $H_2$ is produced in the electrolyser, and diverted to the methanation plant, while the $O_2$ co-produced is used to alleviate the ASU demand, that feeds the BOF and the oxy-BF. The amine scrubbing stage captures $CO_2$ from the BFG, and sends it to the methanation plant, while the clean-BFG is presented with two options (TGR-Split block): it can be blended again with the remaining BFG, or be injected in the tuyeres of the oxy-BF as reducing agent. The methanation plant produces SNG from $CO_2$ and $H_2$, and injects it as reducing agent in the oxy-BF. The BF now operates under oxy-fuel conditions, which means that pure oxygen is injected instead of air. Other heating blocks were represented with the conventional heat exchanger icon (e.g., $O_2$, Clean-BFG or SNG heating), together with the required temperature and the fuel used. The modelling details and methodology for the PtG-steelmaking blocks, as well as for the conventional I&S blocks, were fully explained in Section 3. The main differences between the conventional I&S plant, OBF with SNG injection, and OBF with SNG and TGR injection are shown in Table 2.

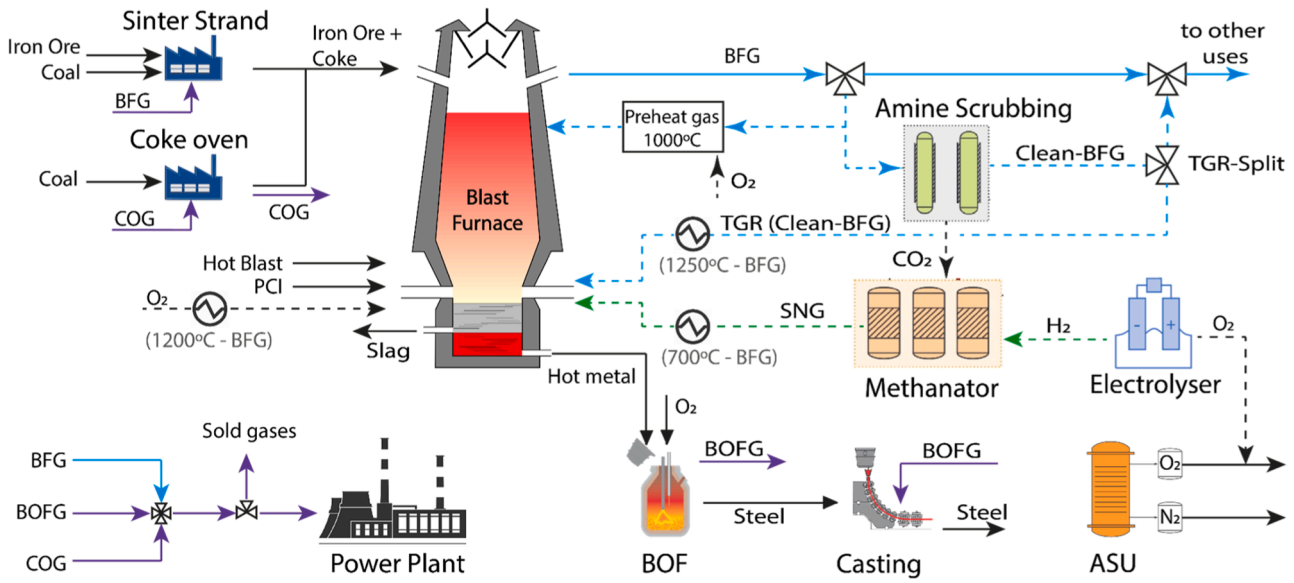


**Fig. 2.** Process flow diagram for conventional iron and steel plant (solid lines) and the integration of power to gas and top gas recycling in an oxygen blast furnace (dashed lines).

**Table 2**
Main data for the description of the conventional I&S plant, OBF with SNG injection, and OBF with SNG and TGR injection.

| | Conventional I&S, serving as benchmark and for Aspen validation [43] | OBF with SNG injection (no TGR) | OBF with SNG and TGR injection |
|---|---|---|---|
| Blast furnace | Conventional BF | Oxygen BF | Oxygen BF |
| Hot blast | Air at 1200 °C | $O_2$ 1200 °C | $O_2$ 1200 °C |
| Auxiliary fuels (tuyeres) | ·Coal | ·SNG: fixed to have 2000 °C AFT | ·TGR: varied from 0 kg/$t_{HM}$ (base case) to 270 kg/$t_{HM}$ (maximum clean-BFG available, which depends on the amine plant size)<br>·SNG: fixed to have 2000 °C AFT (as more TGR is injected, less SNG can be injected) |
| Additional equipment | n/a | ·Methanator: sized to produce the SNG required in the OBF<br>·Electrolyser: sized to produce the $H_2$ required in the methanator<br>·Amine scrubbing; sized to capture the $CO_2$ required in the methanator | ·Methanator: sized to produce the SNG required in the OBF (the higher the TGR injected, the lower the SNG, and the smaller the methanator)<br>·Electrolyser: sized to produce the $H_2$ required in the methanator<br>·Amine scrubbing; sized to capture the $CO_2$ required in the methanator |

## 3. Methodology

The process models for both the conventional I&S and the PtG-steelmaking integration were modelled in Aspen Plus v11. Fig. 2 shows the hierarchy blocks for both case studies, where each block consists of different sub-models and works with its own Aspen property method [46], in order to faithfully reproduce each process. Mass and energy balances of the system are calculated by the software Aspen Plus.

### 3.1. Conventional I&S plant

Solid lines in Fig. 2 represent the conventional I&S plant. The conventional I&S plant serves as a reference model, which has been previously detailed in [43]. The reference case includes several hierarchies, such as the sinter strand, coke oven, blast furnace, basic oxygen furnace, and power plant hierarchies, and the model considers a simplified version of the process (table Table 3). Additional parameters, such as BFG composition and air and coke flow rates, are externally calculated using the extended operating line methodology [36], [44]. CO and $H_2$ utilization are computed using Eqs. (9) and (10), respectively, with each component representing the content present in the blast furnace gas. The utilization of $H_2$ varies widely in the literature, with reported values ranging from 0.3 to 0.54 [47], [48]. In our study, we have opted for a value of 0.47 (if we do not take into account in Eq. (10) the steam from the upper injection, because this $H_2O$ does not come from the reduction of iron oxides, the utilization of $H_2$ is 0.42).

**Table 3**
Input data for the conventional I&S plant modelling.

| Variable | Value | Units |
|---|---|---|
| Coke oven temperature | 1100 | °C |
| $H_2$ utilization (Eq. (10)) | 0.47 | - |
| Carbon content in hot metal | 4.5 | wt% |
| Carbon content in final steel | 0.267 | wt% |
| Power plant size | 100 | MW |

$$\mu_{CO} = CO_2/(CO_2 + CO) \quad (9)$$

$$\mu_{H2} = H_2O/(H_2O + H_2) \quad (10)$$

#### 3.1.1. Model validation

The results and validation of the reference case were previously performed in [43] and can also be found in the supplementary data. The plant was assumed to have a 320 $t_{HM}$/h production rate and the total $CO_2$ emissions of the plant were found to be 1943 $kg_{CO2}/t_{HM}$. The main mass flow rates for the conventional I&S plant simulated in Aspen were compared to typical values from bibliography, and all results agreed

with the literature data, validating the conventional I&S plant model.

### 3.2. PtG-steelmaking integration with TGR

Following subsections show the assumptions made for the oxygen blast furnace (3.2.1), the modelling methodology for the PtG plant (3.2.2), the distribution of combustible gases (3.2.3), the sizing of the PtG plant (3.2.4), the techno-economic indicators (3.2.5).

#### 3.2.1. Oxy-BF

When injecting pure $O_2$ instead of air in the BF, the total bosh gas volume decreases due to the absence of nitrogen, what causes an insufficient preheat of the burden and a low BFG temperature. If the BFG temperature decreases below 100 °C, problems regarding water condensation and oxidation may appear. To solve this problem, a preheating gas injection in the upper part of the furnace was necessary. As preheating gas, it is commonly used BFG which is burned with pure oxygen at 1000 °C [8], [9].

The temperature at which the $O_2$ should be injected in the oxy-BF was already discussed in [45], concluding that hot oxygen injection (1200 °C) obtains greater benefits than cold oxygen injection (25 °C), both technical and economically.

#### 3.2.2. PtG modelling

The power to gas plant considered in this integration consists of a PEM electrolyser, an amine scrubbing and a methanation plant. The amine scrubbing model captures 90% of the inlet $CO_2$, using methyldiethanolamine (50 wt% MDEA and 50 wt% water) as solvent. The absorber column was modelled with 15 stages, and the stripper column with 19 stages. There is also a heat exchanger to recover heat between the lean and rich streams, and a condenser in the $CO_2$ stream exiting the stripper to recover water and solvent dragged in the gas. For the PEM electrolyser, water was fed at ambient conditions and the energy consumption was set to 3.8 kWh/$Nm^3$ [49]. PEM technology was chosen over SOEC (solid oxide electrolysis cell) due to its higher level of commercial development (TRL-7 vs. TRL-5). Additionally, PEM technology was preferred over AEL (alkaline) because it offers greater flexibility in load-following operations with renewable sources [50]. The methanation plant was supplied with green $H_2$ from the electrolyser and $CO_2$ from the amine scrubber, in stoichiometric proportion ($H_2/CO_2$ ratio of 4). Two isothermal fixed-bed reactors worked at 350 and 300 °C respectively, and at constant pressure of 5 bar [51], [52]. An intermediate condensation removed the water at 100 °C. The final SNG was delivered at 25 °C and 5 bar. Additional information on the methodology and validation of the PtG system can be found in [43].

#### 3.2.3. Distribution of combustible gases

The distribution for the combustible gases (BFG, BOFG and COG) remained almost the same, compared with the base case. However, there were noticeable differences, especially for the BFG, as its energy content increased when shifting from BF to oxy-BF.

First, part of the raw BFG was diverted to the preheating gas burner, where it was combusted with pure oxygen and injected at 1000 °C in the upper part of the oxy-BF. Then, part of the BFG passed through the amine scrubbing stage, where the $CO_2$ that feeds the methanation plant is captured. The clean-BFG is divided into two streams (TGR-split block, see Fig. 2): the first one was used as reducing agent in the oxy-BF (i.e., TGR), and the second one was blended with the remaining BFG. The latter was used to feed the remaining thermal needs (sinter strand, $O_2$ heater, clean-BFG heater and SNG heater).

The distribution of the remaining combustible gases, the COG and BOFG, was kept the same, feeding the coke oven and the casting stage. Excess BFG, COG and BOFG were mixed and fed to the power plant or sold to industries nearby, as in the base case.

#### 3.2.4. Sizing of the PtG plant

For the PtG-steelmaking integration with TGR and oxy-BF, several data points were analysed. In all of these data points, the adiabatic flame temperature (AFT) of the furnace should be kept above 2000 °C for technical reasons [53–56], which is a limiting factor when injecting SNG and TGR gases. The first point corresponded to 0 $kg_{TGR}/t_{HM}$, i.e., 0 kg of clean-BFG were directed to the oxy-BF through the TGR-split valve. The gas injected was increased until a maximum is found, corresponding to all the clean-BFG available.

In the first point, the amount of SNG injected was maximum, due to the absence of TGR gas. Thus, the methanation plant, the amine scrubbing and the PEM electrolyser were sized. At this point, the TGR-split valve sent all clean-BFG flow rate to blend with the remaining BFG.

For the next data points, the TGR-split valve divided the clean-BFG flow and sent a certain amount of clean-BFG to the oxy-BF. In order not to drop the AFT below 2000 °C, the SNG flow rate had to be reduced, what also decreased the size of the methanation plant, amine scrubbing and PEM electrolyser. This also meant that, for a given flow rate of TGR gas (i.e., a given flow of clean-BFG derived to the oxy-BF), less clean-BFG was produced in the first place in the amine scrubbing. The last data point studied corresponded to the one where the maximum amount of TGR could be injected, and therefore no clean-BFG was left to be blended with the BFG. At this point, some SNG was also injected, as the $CO_2$ produced in the amine scrubbing was consumed in the methanation stage.

The results in Section 4 were all presented as a function of the TGR mass flow rate (X-axis), where 0 $kg_{TGR}/t_{HM}$ means no TGR was considered, and 270 $kg_{TGR}/t_{HM}$ means that all the clean-BFG was injected in the oxy-BF as reducing agent.

#### 3.2.5. Techno-economic indicators

The technical indicators are the coal-equivalent replacement ratio (coal-e RR) and the energy penalty. The former was defined as the sum of the pulverized coal and coking coal replaced by the SNG and the TGR (Eq. (11)). The latter was defined as the net energy consumed in the industry per kg of $CO_2$ avoided with the PtG-steelmaking integration (Eq. (12)). Units and description of equation variables are in Table 4.

$$Coal-e \quad RR = \frac{\Delta\dot{m}_{PCI} + \Delta\dot{m}_{CokingCoal}}{\Delta\dot{m}_{SNG} + \Delta\dot{m}_{TGR}} \quad \left[kg_{Coal}/kg_{ReducingGas}\right] \tag{11}$$

$$E_{penalty} = \frac{\Delta E_{cons} - \Delta E_{coal} \bullet \eta_{elec} - \Delta E_{gases} \bullet \eta_{elec}}{\Delta\dot{m}_{CO2}} \left[MJ \Big/ kg_{CO_2}\right] \tag{12}$$

The economic indicators are the specific costs, in in €/$t_{CO2}$ and €/$t_{HM}$, see Eq. (13) and Eq. (14). The analysis assumed a loan amortization period of 20 years, a PtG system operating for 8000 h per year [57], and

**Table 4**
Description of variables in Eqs. (9–12).

| Variable | Units | Description |
|---|---|---|
| $\Delta\dot{m}_{PCI}$ | $kg_{PCI}/t_{HM}$ | *Savings in PCI consumption* |
| $\Delta\dot{m}_{CokingCoal}$ | $kg_{CokingCoal}/t_{HM}$ | *Savings in coking coal consumption* |
| $\Delta\dot{m}_{SNG}$ | $kg_{SNG}/t_{HM}$ | *Increase in SNG injection* |
| $\Delta\dot{m}_{TGR}$ | $kg_{TGR}/t_{HM}$ | *Increase in TGR injection* |
| $\Delta E_{cons}$ | $MJ/t_{HM}$ | *Increase in electricity consumption in the industry* |
| $\Delta E_{coal}$ | $MJ/t_{HM}$ | *Savings in coal energy* |
| $\Delta E_{gases}$ | $MJ/t_{HM}$ | *Increase in excess sold gases* |
| $\eta_{elec}$ | - | *Energy conversion factor from coal to electricity (0.33)* |
| CAPEX | *M€* | *Capital Expenditure* |
| OPEX | *M€/year* | *Operational Expenditure* |
| Incomes | *M€/year* | *Operational Incomes* |
| Loan amortization | *Years* | *Process of paying off a loan over time* |
| $CO_2$ avoided | $t_{CO_2}/h$ | *$CO_2$ avoided per hour* |
| Operating hours | $h/year$ | *Operating hours per year* |

a renewable electricity price of 77 €/MWh. A detailed analysis on the CAPEX, OPEX and Incomes can be found in the supplementary data.

$$CO_2\ avoidance\ Cost = \frac{\left(\frac{Capex}{Loan\ amortization} + Opex - Incomes\right)\cdot 10^6}{CO_2\ avoided \cdot Operating\ hours}\ \left[\frac{€}{t_{CO_2}}\right] \quad (13)$$

$$Specific\ Implementatio\ Cost = \frac{\left(\frac{Capex}{Loan\ amortization} + Opex - Incomes\right)\cdot 10^6}{Iron\ Production \cdot Operating\ hours}\ \left[\frac{€}{t_{HRC}}\right] \quad (14)$$

It is worth noting that for the CO2 emission calculation all direct and indirect sources of CO2 have been considered. This includes CO2 emissions from the different processes for steelmaking (sintering, coke oven, etc), the power plant and the sold gases. The CO contained in the BFG is also computed, as it is used as fuel in the sintering or power plant and therefore transformed to CO2.

It's important to highlight that the $CO_2$ emission calculation encompasses all sources, both direct and indirect. This covers $CO_2$ emissions from various steelmaking processes (sintering, coke ovens, etc.), the power plant, and the sale of gases. It is also considered the CO and $CH_4$ within the BFG, BOFG and COG gases, as they are used as fuel in other processes, leading to its conversion into $CO_2$.

## 4. Results and discussion

Sections 4.1, 4.2 and 4.3 document the main results for the PtG-steelmaking integration with TGR and oxy-BF, where all the figures present the data as a function of the TGR mass flow rate ($kg_{clean\text{-}BFG}/t_{HM}$).

### 4.1. PtG integration in TGR-Oxygen blast furnace

Converting the BF to an oxy-BF allowed for higher inputs of reducing agents. In this simulation, SNG was fixed so that the flame temperature was 2000 °C (minimum technical limit). All the PCI and part of the coke were avoided thanks to the synthetic gas. At this operating point, we progressively shifted the SNG injection to TGR injection. Fig. 3 shows the amount of reducing agents injected in the oxy-BF (coke, SNG and TGR), and the coal-e RR of the gaseous reducing agents, as the SNG is replaced by TGR. The SNG consists mainly of methane (94.7% $CH_4$), with minor components comprising 3.9% $H_2$, 1.0% $CO_2$ and 0.4% $H_2O$. The total flow of reducing agents increased, while the coal-e RR decreased, with the TGR. This suggests that the TGR is not as good reducing agent as the SNG. Nevertheless, despite the coal-e RR decreased rapidly, it only resulted in a slight increase in the coke rate (279–300 $kg_{coke}/t_{HM}$). The reason can be found in Eq. (11), where the numerator barely changed, but the denominator increased remarkably (per each kg of SNG replaced, 3.1–3.4 kg of TGR were added).

When increasing the TGR gas, a drop in the $H_2$ content in the BFG was observed, compensated by an increase in the CO and $CO_2$ content (see Fig. 4). The reason is the lower H:C ratio of the TGR (approx. 0.5–0.8) compared to that of SNG (approx. 4). The decrease in the $H_2$ content, and the increase in the $CO_2$ content, made the lower heating value (LHV) of the BFG to diminish. However, the higher amount of reducing agents also led to a higher BFG mass flow rate. Both effects counterbalanced each other, resulting in a nearly constant BFG energy content (referred to the total energy content, before recirculations), as shown in Fig. 4.

Despite the increase in CO and $CO_2$ in the BFG, the CO utilization ratio (Eq. (9)) hardly varied, ranging between 50.0% and 51.7% for all data points. The preheating gas injected in the upper part of the oxy-BF was also considered, but its influence was very small since it remained constant at 205–207 $kg/t_{HM}$, allowing the BFG temperature to not fall below 150 °C.

### 4.2. Thermal energy integration and energy penalty

The amine scrubber captured 90% of the $CO_2$ contained in the BFG, with a $CO_2$ purity of 95%, and a specific heat consumption of 3.1 $MJ/kg_{CO2}$. The methanation plant produced SNG at 5 bar and with 95 vol% of $CH_4$, releasing 6.1 $MJ/kg_{CO2}$. No solid carbon deposition was found in the methanation plant.

When integrating the PtG technology, new thermal streams had to be considered. The isothermal methanation plant generated heat at 300–350 °C, while the stripper of the amine scrubber required heat at 110–130 °C, so the heat consumption of the amine scrubbing could be covered by the exothermal heat released by the methanation. Perpiñán et al. [43] demonstrated through a pinch analysis the technical feasibility of supplying the heat demand of an amine scrubbing plant (3.7 $MJ/kg_{CO2}$) with the exothermal heat of an isothermal methanation plant (6.1 $MJ/kg_{CO2}$). In this simulation, the same amount of heat was released by the methanation, and less thermal consumption was found in the amine scrubbing (3.1 $MJ/kg_{CO2}$), so the technical viability for this thermal integration is guaranteed.

As the TGR gas increased, less SNG was injected into the oxy-BF,

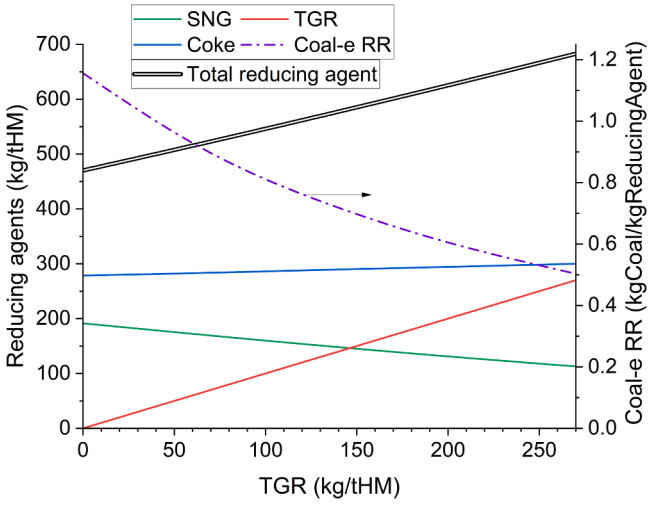


**Fig. 3.** Reducing agents in the OBF (SNG, green line; TGR, red line; coke, blue line; total reducing agents, black line) and coal-e RR (purple dashed line) as a function of the TGR mass flow injected in the OBF.

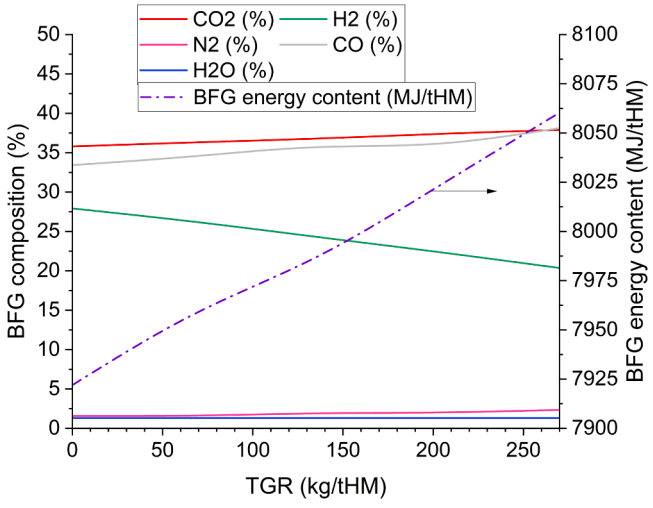


**Fig. 4.** BFG composition ($CO_2$, red line; $H_2$, green line; $N_2$, pink line; CO, grey line; $H_2O$, blue line) and BFG energy content (purple dashed line) as a function of the amount of TGR mass flow injected in the OBF.

what lowers the size of the methanation plant and the electrolyser. The PEM size decreased from 1268 MW to 741 MW when injecting 270 $kg_{TGR}/t_{HM}$. However, the lower the electrolyser size, the lower the oxygen by-produced, leading to an oxygen deficit for TGR flows higher than 190 $kg_{TGR}/t_{HM}$. This should be covered by an ASU plant (see Fig. 5).

The $CO_2$ emission reduction for the PtG-steelmaking integration ranged between 30% and 34% (Fig. 6). Higher emission reduction was found without TGR injection, due to the higher coal-e RR at this point (see Fig. 3). The total emissions decreased from 1943 $kg_{CO2}/t_{HM}$ to 1279 and 1361 $kg_{CO2}/t_{HM}$, compared to the conventional BF, when integrating PtG and TGR technologies, respectively. The $CO_2$ recycled through methanation ranged between 305 and 517 $kg_{CO2}/t_{HM}$, which would otherwise be emitted to the atmosphere.

The electricity consumption, sold gases and energy penalty are shown in Fig. 7. The electricity consumption had a mostly linear dependency on the PEM electrolyser, as its consumption accounted for 88–92% of all the electricity consumed in the industry. The maximum electricity consumption was 15,581 $MJ/t_{HM}$ (no TGR), which could be reduced to 9548 $MJ/t_{HM}$ if TGR gas was used. However, it still represented an increase of 16 times and 10 times in the total electricity consumption, respectively, compared to the conventional BF (950 $MJ/t_{HM}$). For TGR flow rates above 190 $kg_{TGR}/t_{HM}$, the ASU started working and consuming electricity, yet the total electricity consumption was barely affected and continued its decreasing trend. The ASU electricity consumption was very low compared to that of the electrolyser. The electricity production in the power plant was the same as for the conventional BF, 1122 $MJ/t_{HM}$ (100 MW).

The sold gases (BFG, COG and BOFG) decreased from 4471 to 1143 $MJ/t_{HM}$ when using TGR gas as reducing agent in the oxy-BF, because of the high fraction of BFG used as TGR (in the conventional I&S plant, the energy sold as combustible gases was 2400 $MJ/t_{HM}$). The energy penalty considers the increase in the electricity consumed, the sold gases and the coal savings. When injecting TGR gas, despite the less energy sold with the steel gases, and the lower coal savings, the energy penalty offered better results. This is because the electricity consumption of the electrolyser rules the energy penalty. The energy penalty was 17 $MJ/t_{HM}$ when injecting SNG alone, and 12 $MJ/t_{HM}$ when also injecting TGR gas.

### 4.3. Economic analysis

The specific carbon capture (CC) cost is shown in Fig. 8, where the red line represents the cost in terms of €/$t_{HM}$ and the black line represents the cost in terms of €/$t_{CO2}$. For higher TGR gas rates, lower CC costs

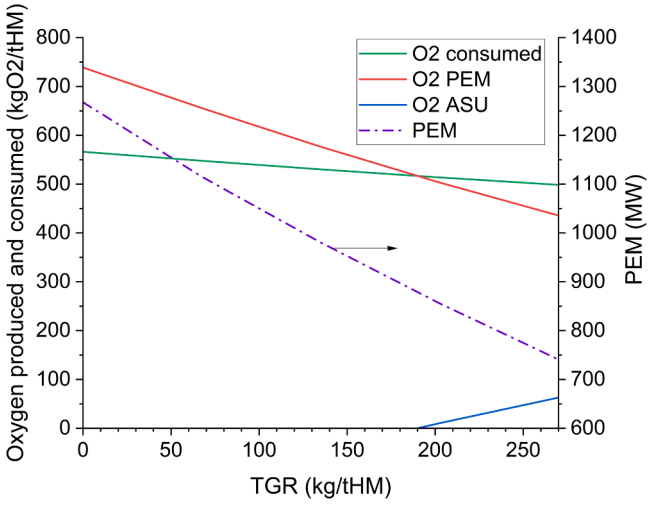


**Fig. 5.** Oxygen produced in the PEM (red line) and in the ASU (blue line), oxygen consumed in the industry (green line) and PEM capacity (purple dashed line) as a function of the amount of TGR mass flow injected in the OBF.

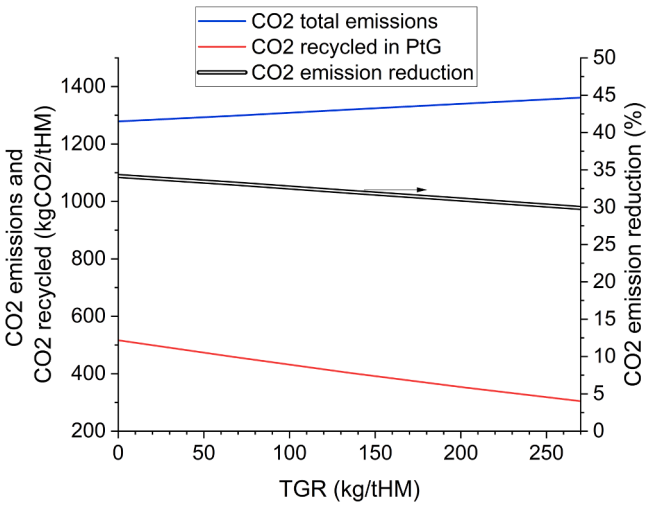


**Fig. 6.** Total $CO_2$ emissions (blue line), $CO_2$ recycled in the PtG system (red line), and percentage of $CO_2$ emission reduction compared to conventional BF (black line) as a function of the amount of TGR mass flow injected in the OBF.

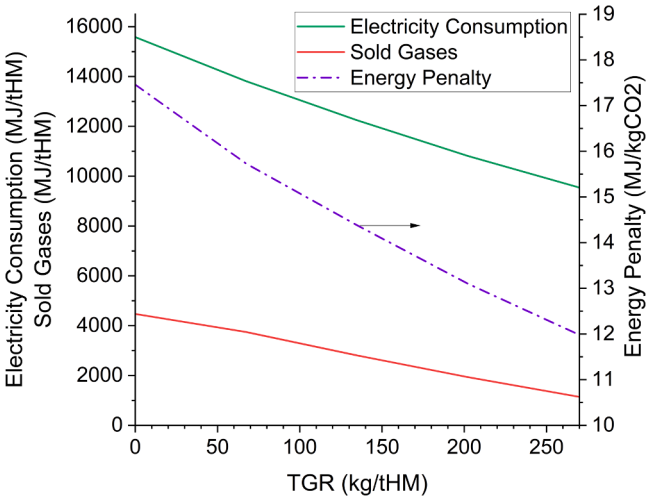


**Fig. 7.** Electricity consumption (green line), sold gases (red line) and energy penalty (purple dashed line) as a function of the amount of TGR mass flow injected in the OBF.

were found, because of the lower electrolyser size and the lower electricity consumption. The PEM accounted for 38–43% of the CAPEX and the electricity for 94–95% of the OPEX. The steel price in 2022 was between 660 and 1400 €/$t_{HRC}$, so the specific CC cost represents an increase of 9–35% in the final product.

For the operation with 270 $kg_{TGR}/t_{HM}$ injected in the oxy-BF, a sensitivity analysis of the specific CC costs (in €/$t_{CO2}$) was performed. The $CO_2$ taxes and the electricity price were varied, looking for those combinations that make the PtG-steelmaking integration economically viable (Fig. 9). Today, with an electricity price of 77 €/MWh and a $CO_2$ tax of 84 €/$t_{CO2}$, the specific CC cost is 216 €/$t_{CO2}$. Negative costs (i.e., actual benefits) could be achieved under some conditions. For a specific CC cost of 0 €/$t_{CO2}$, a maximum electricity price of 21 €/MWh should be paid, or a minimum $CO_2$ tax of 300 €/$t_{CO2}$ should apply. However, these prices or taxes do not guarantee a profitable investment, since the CAPEX should also be amortized. To amortize CAPEX in 20 years (i.e., total investment pay-back of 20 years), the electricity price should be 18 €/MWh, or the $CO_2$ tax 313 €/$t_{CO2}$, or an intermediate combination of both parameters, coinciding with a specific CC cost of − 13 €/$t_{CO2}$ or − 8 €/$t_{HM}$. With an electricity price of 35 €/MWh (cost of production for

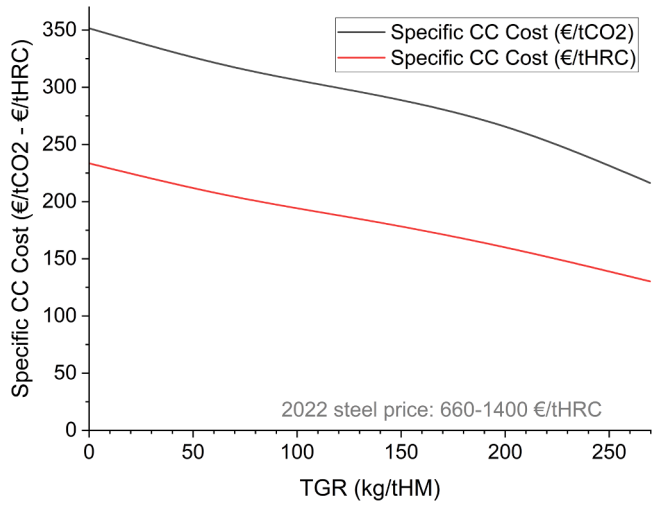


**Fig. 8.** Specific carbon capture (CC) cost in €/$t_{CO2}$ (black line) and €/$t_{HRC}$ (red line) as a function of the amount of TGR mass flow injected in the OBF (2022 steel price [58]).

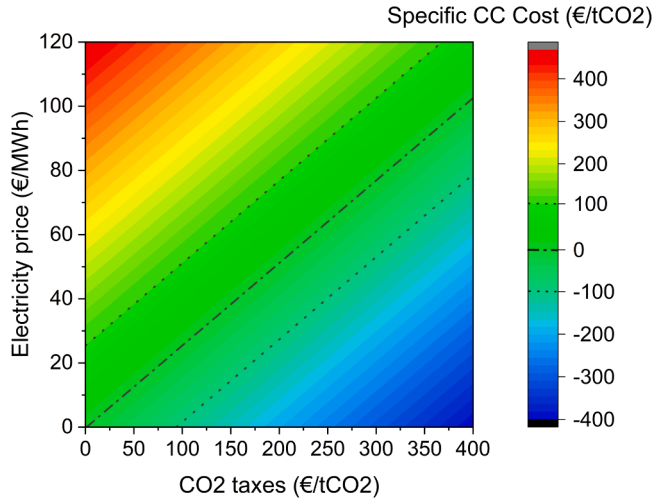


**Fig. 9.** Specific CC cost in €/$t_{CO2}$ as a function of the $CO_2$ taxes and the electricity price for an OBF with two auxiliary fuel injections (113 $kg_{SNG}/t_{HM}$ and 270 $kg_{TGR}/t_{HM}$), an electrolyser of 741 MW, and an amine scrubbing of 305 $kg_{CO2}/t_{HM}$.

wind power [59]), and a $CO_2$ tax of 150 €/$t_{CO2}$, the pay-back is 20 years and the investment would be profitable.

For illustration purposes, Table 5 compares results for two different data points: only SNG injection and maximum TGR gas injection. It can be seen that the first data point offered better environmental results, such as higher $CO_2$ emission reduction and lower coke rate in the OBF. However, similar environmental results were found in the second data point but offering further benefits, such as lower PEM size, energy penalty and costs. For these reasons, whenever possible, TGR is a technology that should be considered along with PtG technology.

## 5. Conclusions

A new concept integrating power to gas and BF top gas recycling with an oxy-BF was presented in this study for $CO_2$ emissions reduction and utilization in the iron and steel industry. Green $H_2$ was produced in an electrolyser with renewable electricity, $CO_2$ was obtained from the BFG through an amine scrubbing stage, and synthetic natural gas is produced from the two previous components in an isothermal methanation plant.

**Table 5**
Main results and comparison for (i) only SNG injection and (ii) maximum TGR gas injection, in an OBF.

| Variable | Units | OBF with SNG injection (no TGR) | OBF with SNG and TGR injection |
|---|---|---|---|
| SNG mass flow rate | $kg/t_{HM}$ | 192 | 113 |
| TGR mass flow rate | $kg/t_{HM}$ | 0 | 270 |
| Coke mass flow rate | $kg/t_{HM}$ | 288 | 300 |
| Total reducing agents | $kg/t_{HM}$ | 470 | 683 |
| PEM size | MW | 1115 | 741 |
| $CO_2$ emission reduction | % | 34.4 | 29.9 |
| Energy penalty | $MJ/t_{HM}$ | 17.5 | 12.0 |
| Cost | €/$t_{CO2}$ | 352 | 216 |
| Cost | €/$t_{HM}$ | 233 | 130 |

The synthetic methane was injected into the OBF on its own or mixed with some clean-BFG (recycled top gas, after $CO_2$ separation). This integration was compared with a conventional BF-BOF iron and steel process. Both simulations, the conventional and the PtG-integration, were modelled in Aspen Plus.

The oxygen by-produced in the electrolyser was almost sufficient to satisfy the oxygen demand in the plant, including the oxygen for the BOF, the preheating gas, and the oxy-BF. Only when the TGR gas was above 190 $kg_{TGR}/t_{HM}$ (i.e., when the PEM capacity was lower than 880 MW), the ASU had to produce a small portion of the overall oxygen demand. The LHV of the BFG decreased when injecting TGR gas, but the mass flow rate increased, resulting in a nearly constant BFG energy content (in $MJ/t_{HM}$).

When injecting SNG in the OBF, 34.4% and 33.1% of the total $CO_2$ emissions and coal consumption were saved, respectively. Due to the lower coal-e RR of the TGR compared to that of the SNG, less $CO_2$ and coal were saved when injecting both reducing agents in the OBF; 29.9% and 28.9% respectively. However, the joint injection of SNG and TGR offered other relevant advantages. For instance, the PEM electrolyser size was greatly reduced, from 1115 to 741 MW, providing additional benefits. As the PEM size decreased, the electricity consumed was also lower, diminishing the energy penalty and the costs, from 17.5 to 12.0 $MJ/t_{HM}$ and from 352 to 216 €/$t_{CO2}$, respectively. However, under certain combinations of $CO_2$ tax, electricity price or economic subsidies, economic profitability could be achieved.

This PtG-steelmaking configuration recycles $CO_2$ via methanation, and CO via TGR. Contrary to other studies that only recycle CO, this configuration is able to supply all downstream thermal energy needs of the steel plant (i.e., the sintering, power plant and other processes). As downstream energy needs were always covered, there was a certain amount of steel gases sold. These sold gases accounted for 4471 $MJ/t_{HM}$ when injecting SNG, and 1143 $MJ/t_{HM}$ when injecting both reducing agents (SNG and TGR).

Technical limitations for this PtG-integration with TGR include the feasibility of the OBF and the TGR, which are technologies still under development, along with the necessity for addressing dynamics and transient effects. Moreover, the on-site configuration of each specific industry may affect the practical implementation of the energy integration, including heat integration. Additionally, the integration of a GW scale electrolyser into the I&S industry raises concerns about various factors such as the availability of renewable electricity in the region or the feasibility of the supply line to the plant. Economic limitations include prices for the $CO_2$ tax and the electricity, as these two variables had a great impact on the specific CC costs and the pay-back. Future research should explore these aspects further to ensure the practicality and viability of large-scale implementation.

To sum up, this novel concept of PtG-integration with TGR in the I&S industry has the potential to recycle $CO_2$ via methanation and CO via TGR, thus reducing $CO_2$ emissions and coal consumption without the need for geological storage. Despite the slightly lower $CO_2$ and coal savings, injection of both SNG and TGR is preferred over the injection of SNG alone, because of the lower energy penalty and costs found. Additionally, the downstream energy needs are always covered, and a certain amount of steel gases are sold (what would not happen if only TGR is applied).

## CRediT authorship contribution statement

**Jorge Perpiñán:** Conceptualization, Methodology, Formal analysis, Visualization, Software, Writing - original draft. **Manuel Bailera:** Conceptualization, Methodology, Visualization, Supervision, Funding acquisition, Project administration, Software, Writing - review & editing. **Begoña Peña:** Conceptualization, Methodology, Supervision, Project administration, Funding acquisition, Writing - review & editing. **Pravin Kannan:** Writing - review & editing. **Valerie Eveloy:** Project administration, Funding acquisition, Writing - review & editing. **Luis M. Romeo:** Project administration, Funding acquisition, Writing - review & editing.

## Declaration of Competing Interest

The authors declare that they have no known competing financial interests or personal relationships that could have appeared to influence the work reported in this paper.

## Data Availability

Data will be made available on request.

## Acknowledgements

The work presented in this paper has been supported by the Khalifa University project CIRA-2020-080. This work has also received funding from the European Union's Horizon 2020 research and innovation program under the Marie Sklodowska-Curie grant agreement no. 887077. This work is part of the R&D project PID2021-126164OB-I00, funded by MCIN/AEI/10.13039/501100011033/ and by the "ERDF A way of making Europe". This research is co-funded by the University of Zaragoza, Fundación Bancaria Ibercaja, and Fundación CAI, through the program "Programa Ibercaja-Cai Estancias de Investigación", nº IT 16/12. Manuel Bailera acknowledges Waseda University, Tokyo, and K1-MET GmbH, Linz.

## Appendix A. Supporting information

Supplementary data associated with this article can be found in the online version at doi:10.1016/j.jcou.2023.102634.

## References

[1] IEA, 2022. "World Energy Outlook 2022," Paris. License: CC BY 4.0 (report); CC BY NC SA 4.0 (Annex A), 2022.
[2] World Steel Association, "WorldSteel." ⟨https://worldsteel.org/steel-topics/statistics/world-steel-in-figures-2022/⟩.
[3] World Economid Forum, "Report on 'The Net-Zero Industry Tracker.'" [Online]. Available: ⟨https://worldsteel.org/steel-topics/statistics/world-steel-in-figures-2022/⟩.
[4] EUROFER, 2023 "A steel roadmap for a low carbon europe 2050, the European Steel Association EUROFER. Brussels, Belgium.," 2013. ⟨https://www.eurofer.eu/assets/publications/archive/archive-of-older-eurofer-documents/2013-Roadmap.pdf⟩ (Accessed Feb. 26, 2023).
[5] M. Wörtler, P. Dahlmann, F. Schuler, H.B. Lüngen, and N. Voigt, 2023. "Steel's contribution to a low-carbon Europe 2050-Technical and economic analysis of the sector's CO2 abatement potential.," 2013. ⟨https://www.bcg.com/de-de/⟩ (Accessed Apr. 26, 2022).
[6] D. Fu, G. Tang, Y. Zhao, J. D'Alessio, C.Q. Zhou, Modeling of iron ore reactions in blast furnace, Int. J. Heat. Mass Transf. vol. 103 (2016) 77–86, https://doi.org/10.1016/j.ijheatmasstransfer.2016.06.060.
[7] H. Kildahl, L. Wang, L. Tong, Y. Ding, Cost effective decarbonisation of blast furnace – basic oxygen furnace steel production through thermochemical sector coupling, J. Clean. Prod. vol. 389 (March 2022) (2023), 135963, https://doi.org/10.1016/j.jclepro.2023.135963.
[8] T. Ariyama, M. Sato, T. Nouchi, K. Takahashi, Evolution of blast furnace process toward reductant flexibility and carbon dioxide mitigation in steel works, ISIJ Int vol. 56 (10) (2016) 1681–1696, https://doi.org/10.2355/isijinternational.ISIJINT-2016-210.
[9] M. Sato, K. Takahashi, T. Nouchi, T. Ariyama, Prediction of next-generation ironmaking process based on oxygen blast furnace suitable for $CO_2$ mitigation and energy flexibility, ISIJ Int. vol. 55 (10) (2015) 2105–2114, https://doi.org/10.2355/isijinternational.ISIJINT-2015-264.
[10] A. Babich and D. Senk, 2015. Recent developments in blast furnace iron-making technology, 2015, p. 505–547. doi:10.1016/B978–1-78242–156-6.00017–4.
[11] W. Zhang, J. Dai, C. Li, X. Yu, Z. Xue, H. Saxén, A review on explorations of the oxygen blast furnace process, Steel Res. Int. vol. 92 (1) (2021), https://doi.org/10.1002/srin.202000326.
[12] M. Bailera, P. Lisbona, B. Peña, L.M. Romeo, A review on $CO_2$ mitigation in the Iron and Steel industry through Power to X processes, J. $CO_2$ Util. vol. 46 (November 2020) (2021), 101456, https://doi.org/10.1016/j.jcou.2021.101456.
[13] M. Abdul Quader, S. Ahmed, S.Z. Dawal, Y. Nukman, Present needs, recent progress and future trends of energy-efficient Ultra-Low Carbon Dioxide ($CO_2$) steelmaking (ULCOS) program, Renew. Sustain. Energy Rev. vol. 55 (. 2016) 537–549, https://doi.org/10.1016/J.RSER.2015.10.101.
[14] R.K. Sahu, S.K. Roy, P.K. Sen, Applicability of top gas recycle blast furnace with downstream integration and sequestration in an integrated steel plant, Steel Res. Int. vol. 1 (5) (2015) 502–516, https://doi.org/10.1002/srin.201400196.
[15] W. Zhang, J. Zhang, Z. Xue, Exergy analyses of the oxygen blast furnace with top gas recycling process, Energy vol. 121 (2017) 135–146, https://doi.org/10.1016/j.energy.2016.12.125.
[16] W. Zhang, Z. Xue, J. Zhang, W. Wang, C. Cheng, Z. Zou, Medium oxygen enriched blast furnace with top gas recycling strategy, J. Iron Steel Res. Int. vol. 24 (8) (. 2017) 778–786, https://doi.org/10.1016/S1006-706X(17)30117-6.
[17] J. Perpiñán, M. Bailera, L.M. Romeo, B. Peña, V. Eveloy, $CO_2$ recycling in the iron and steel industry via power-to-gas and oxy-fuel combustion, Energies vol. 14 (21) (2021) 7090, https://doi.org/10.3390/en14217090.
[18] J. van der Stel, G. Louwerse, D. Sert, A. Hirsch, N. Eklund, M. Pettersson, Top gas recycling blast furnace developments for 'green' and sustainable ironmaking, Ironmak. Steelmak. vol. 40 (7) (. 2013) 483–489, https://doi.org/10.1179/0301923313Z.000000000221.
[19] P. Jin, Z. Jiang, C. Bao, S. Hao, X. Zhang, The energy consumption and carbon emission of the integrated steel mill with oxygen blast furnace, Resour. Conserv. Recycl. vol. 117 (2017) 58–65, https://doi.org/10.1016/j.resconrec.2015.07.008.
[20] J. Perpiñán, et al., Integration of carbon capture technologies in blast furnace based steel making: a comprehensive and systematic review, Fuel (2022), https://doi.org/10.1016/j.fuel.2022.127074.
[21] G. Danloy, et al., ULCOS - pilot testing of the low-$CO_2$ Blast Furnace process at the experimental BF in Lulea, Rev. Metall. Cah. D'Informations Tech. vol. 106 (1) (2009) 1–8, https://doi.org/10.1051/metal/2009008.
[22] A. Arasto, E. Tsupari, J. Kärki, J. Lilja, M. Sihvonen, Oxygen blast furnace with $CO_2$ capture and storage at an integrated steel mill-Part I: Technical concept analysis, Int. J. Greenh. Gas. Control vol. 30 (2014) 140–147, https://doi.org/10.1016/j.ijggc.2014.09.004.
[23] E. Tsupari, J. Kärki, A. Arasto, J. Lilja, K. Kinnunen, M. Sihvonen, Oxygen blast furnace with $CO_2$ capture and storage at an integrated steel mill - Part II: Economic feasibility in comparison with conventional blast furnace highlighting sensitivities, Int. J. Greenh. Gas. Control vol. 32 (2015) 189–196, https://doi.org/10.1016/j.ijggc.2014.11.007.
[24] Y. Ohno, M. Matsuura, H. Mitsufuji, T. Furukawa, Process characteristics of a commercial-scale oxygen blast furnace process with shaft gas injection, ISIJ Int. vol. 32 (7) (1992) 838–847, https://doi.org/10.2355/isijinternational.32.838.
[25] W. Zhang, J. Zhang, Z. Xue, Z. Zou, Y. Qi, Unsteady analyses of the top gas recycling oxygen blast furnace, ISIJ Int vol. 56 (8) (2016) 1358–1367, https://doi.org/10.2355/isijinternational.ISIJINT-2016-090.
[26] A. Arasto, E. Tsupari, J. Kärki, E. Pisilä, L. Sorsamäki, Post-combustion capture of $CO_2$ at an integrated steel mill - Part I: technical concept analysis, Int. J. Greenh. Gas. Control vol. 16 (2013) 271–277, https://doi.org/10.1016/j.ijggc.2012.08.018.
[27] A. Arasto, E. Tsupari, J. Kärki, M. Sihvonen, J. Lilja, Costs and potential of carbon capture and storage at an integrated steel mill, Energy Procedia vol. 37 (2013) 7117–7124, https://doi.org/10.1016/j.egypro.2013.06.648.
[28] E. Tsupari, J. Kärki, A. Arasto, E. Pisilä, Post-combustion capture of $CO_2$ at an integrated steel mill - Part II: economic feasibility, Int. J. Greenh. Gas. Control vol. 16 (2013) 278–286, https://doi.org/10.1016/j.ijggc.2012.08.017.
[29] D.E. Wiley, M.T. Ho, A. Bustamante, Assessment of opportunities for $CO_2$ capture at iron and steel mills: an Australian perspective, Energy Procedia vol. 4 (2011) 2654–2661, https://doi.org/10.1016/j.egypro.2011.02.165.
[30] M.A. Quader, S. Ahmed, R.A. Raja Ghazilla, S. Ahmed, M. Dahari, Evaluation of criteria for $CO_2$ capture and storage in the iron and steel industry using the 2-tuple DEMATEL technique, J. Clean. Prod. vol. 120 (2016) 207–220, https://doi.org/10.1016/J.JCLEPRO.2015.10.056.
[31] M. Biermann, H. Ali, M. Sundqvist, M. Larsson, F. Normann, F. Johnsson, Excess heat-driven carbon capture at an integrated steel mill – Considerations for capture

cost optimization, Int. J. Greenh. Gas. Control vol. 91 (September) (2019), 102833, https://doi.org/10.1016/j.ijggc.2019.102833.
[32] F.A. Tobiesen, H.F. Svendsen, T. Mejdell, Modeling of blast furnace $CO_2$ capture using amine absorbents, Ind. Eng. Chem. Res. vol. 46 (23) (2007) 7811–7819, https://doi.org/10.1021/ie061556j.
[33] H. Kim, J. Lee, S. Lee, I.B. Lee, J. hyoung Park, J. Han, Economic process design for separation of $CO_2$ from the off-gas in ironmaking and steelmaking plants, Energy vol. 88 (. 2015) 756–764, https://doi.org/10.1016/J.ENERGY.2015.05.093.
[34] S. Yun, M.G. Jang, J.K. Kim, Techno-economic assessment and comparison of absorption and membrane $CO_2$ capture processes for iron and steel industry, Energy vol. 229 (2021), 120778, https://doi.org/10.1016/j.energy.2021.120778.
[35] M. Onoda, Y. Matsuzaki, F.A. Chowdhury, H. Yamada, K. Goto, S. Tonomura, Sustainable aspects of ultimate reduction of $CO_2$ in the steelmaking process (COURSE50 Project), Part 2: $CO_2$ capture, J. Sustain. Metall. vol. 2 (3) (2016) 209–215, https://doi.org/10.1007/s40831-016-0067-3.
[36] M. Bailera, T. Nakagaki, and R. Kataoka, 2021. "Revisiting the Rist diagram for predicting operating conditions in blast furnaces with multiple injections," 2021, doi:10.12688/openreseurope.14275.1.
[37] D.C. Rosenfeld, H. Böhm, J. Lindorfer, M. Lehner, Scenario analysis of implementing a power-to-gas and biomass gasification system in an integrated steel plant: a techno-economic and environmental study, Renew. Energy vol. 147 (2020) 1511–1524, https://doi.org/10.1016/j.renene.2019.09.053.
[38] A.R. Medved, M. Lehner, D.C. Rosenfeld, J. Lindorfer, K. Rechberger, Enrichment of integrated steel plant process gases with implementation of renewable energy Integration of power-To-gas and biomass gasification system in steel production, Johns. Matthey Technol. Rev. vol. 65 (3) (2021) 453–465, https://doi.org/10.1595/205651321x16161444481140.
[39] S. Hisashige, T. Nakagaki, T. Yamamoto, $CO_2$ emission reduction and exergy analysis of smart steelmaking system adaptive for flexible operating conditions, ISIJ Int vol. 59 (4) (2019) 598–606, https://doi.org/10.2355/isijinternational.ISIJINT-2018-355.
[40] V. Shatokha, Modeling of the effect of hydrogen injection on blast furnace operation and carbon dioxide emissions, Int. J. Miner. Metall. Mater. vol. 29 (10) (2022) 1851–1861, https://doi.org/10.1007/s12613-022-2474-8.
[41] J. Kim, et al., An integrative process of blast furnace and SOEC for hydrogen utilization: techno-economic and environmental impact assessment, Energy Convers. Manag. vol. 250 (August) (2021), 114922, https://doi.org/10.1016/j.enconman.2021.114922.
[42] M. Bailera, T. Nakagaki, R. Kataoka, Limits on the integration of power to gas with blast furnace ironmaking, Elsevier, 2022, https://doi.org/10.1016/J.JCLEPRO.2022.134038.
[43] J. Perpiñán, M. Bailera, B. Peña, L.M. Romeo, V. Eveloy, Technical and economic assessment of iron and steelmaking decarbonization via power to gas and amine scrubbing, Energy vol. 276 (2023), https://doi.org/10.1016/j.energy.2023.127616.
[44] M. Bailera, T. Nakagaki, R. Kataoka, Extending the operating line methodology to consider shaft and preheating injections in blast furnaces, ISIJ Int vol. 62 (12) (2022) 1–12, https://doi.org/10.2355/isijinternational.ISIJINT-2022-111.
[45] J. Perpiñán, M. Bailera, B. Peña, L.M. Romeo, V. Eveloy, High oxygen and SNG injection in blast furnace steelmaking with power to gas integration and $CO_2$ recycling, J. Clean. Prod. (2023), https://doi.org/10.1016/j.jclepro.2023.137001.
[46] Aspen Technology Inc., 2019. "Aspen Physical Property Methods - Reference Manual." AspenTech, 2019.
[47] Y. Chen, H. Zuo, Review of hydrogen-rich ironmaking technology in blast furnace, Ironmak. Steelmak. vol. 48 (6) (2021) 749–768, https://doi.org/10.1080/03019233.2021.1909992.
[48] C. Lan, Y. Hao, J. Shao, S. Zhang, R. Liu, Q. Lyu, Effect of H2 on blast furnace ironmaking: a review, Metals vol. 12 (11) (2022), https://doi.org/10.3390/met12111864.
[49] "NEL Hydrogen", 2019. https://nelhydrogen.com/ (Accessed Mar. 02, 2022).
[50] M.N.I. Salehmin, T. Husaini, J. Goh, A.B. Sulong, High-pressure PEM water electrolyser: a review on challenges and mitigation strategies towards green and low-cost hydrogen production, Energy Convers. Manag. vol. 268 (June) (2022), 115985, https://doi.org/10.1016/j.enconman.2022.115985.
[51] K. Izumiya and I. Shimada, 2021. "K2- Methane Producing Technology from CO 2 for Carbon Recycling." pp. 34–35, 2021.
[52] S. Rönsch, et al., Review on methanation - From fundamentals to current projects, Fuel vol. 166 (2016) 276–296, https://doi.org/10.1016/j.fuel.2015.10.111.
[53] K.S. Abdel Halim, V.N. Andronov, M.I. Nasr, Blast furnace operation with natural gas injection and minimum theoretical flame temperature, Ironmak. Steelmak. vol. 36 (1) (2009) 12–18, https://doi.org/10.1179/174328107X155240.
[54] K.S.A. Halim, Theoretical approach to change blast furnace regime with natural gas injection, J. Iron Steel Res. Int. vol. 20 (9) (2013) 40–46, https://doi.org/10.1016/S1006-706X(13)60154-5.
[55] K.S. Abdel Halim, Effective utilization of using natural gas injection in the production of pig iron, Mater. Lett. vol. 61 (14–15) (2007) 3281–3286, https://doi.org/10.1016/j.matlet.2006.11.053.
[56] J.G. Peacey and W.G. Davbenport, 1979. The Iron Blast Furnace. Theory and Practice (1979). 1979. doi: ISBN 0–08-023258–2.
[57] M. Bailera, S. Espatolero, P. Lisbona, L.M. Romeo, Power to gas-electrochemical industry hybrid systems: a case study, Appl. Energy vol. 202 (2017) (2017) 435–446, https://doi.org/10.1016/j.apenergy.2017.05.177.
[58] "Marketwatch web page (HRC steel)," 2022. https://www.marketwatch.com/investing/index/steel?countryCode=XX (accessed Jul. 25, 2022).
[59] "IRENA," , 2022. ⟨https://www.irena.org/costs/Power-Generation-Costs⟩ (Accessed May 10, 2022).